Three-dimensional magnetic fields of molecular clouds

Mehrnoosh Tahani [1,2,*]

[1] *Banting and KIPAC Fellow: Kavli Institute for Particle Astrophysics & Cosmology (KIPAC), Stanford University, Stanford, CA 94305, USA*
[2] *Covington Fellow: Dominion Radio Astrophysical Observatory, Herzberg Astronomy and Astrophysics Research Centre, National Research Council Canada, P. O. Box 248, Penticton, BC V2A 6J9 Canada*

Correspondence*:
Mehrnoosh Tahani
mtahani@stanford.edu

ABSTRACT

To investigate the role of magnetic fields in the evolution of the interstellar medium, formation and evolution of molecular clouds, and ultimately the formation of stars, their three-dimensional (3D) magnetic fields must be probed. Observing only one component of magnetic fields (along the line of sight or parallel to the plane of the sky) is insufficient to identify these 3D vectors. In recent years, novel techniques for probing each of these two components and integrating them with additional data (from observations or models), such as Galactic magnetic fields or magnetic field inclination angles, have been developed, in order to infer 3D magnetic fields. We review and discuss these advancements, their applications, and their future direction.

1 INTRODUCTION

The Gaia mission (Gaia Collaboration et al., 2016), particularly with its stellar parallax distances (Luri et al., 2018) and radial velocities (Soubiran et al., 2018), has enabled significant advances in various areas of astrophysics, ranging from the Galaxy structure (e.g., Kounkel and Covey, 2019) and evolution (e.g., Poggio et al., 2020; Ruiz-Lara et al., 2020) to binary systems (Wyrzykowski et al., 2020). Thanks to Gaia, the three-dimensional (3D) density field of the Galaxy, especially of nearby molecular clouds (Großschedl et al., 2018; Zucker et al., 2021; Rezaei Kh. et al., 2020; Rezaei Kh. and Kainulainen, 2022) and the solar neighborhood (e.g., Zucker et al., 2022), can now be mapped, enabling us to study the interstellar medium (ISM) evolution (e.g., Bialy et al., 2021; Kounkel et al., 2022). However, studies of the ISM evolution are incomplete without observing 3D magnetic fields, as the two are interdependent (e.g., Tahani et al., 2022b; Kounkel et al., 2022).

Magnetic fields influence the star-formation process, from the evolution of diffuse ISM (Haverkorn, 2015) and formation of molecular clouds (e.g., Iwasaki et al., 2019) to formation of sub-structures and stars (e.g., Pattle et al., 2022, and references therein). However, their role remains undetermined (e.g, Hennebelle and Inutsuka, 2019; Krumholz and Federrath, 2019). Magnetic fields can stabilize the clouds against gravity (e.g., Fiege and Pudritz, 2000a,b), allow for the formation of denser structures and stars (e.g., Inoue et al., 2018), reduce the star-formation rate (see Hennebelle and Inutsuka, 2019, and references therein), or regulate gas flow (e.g., Seifried and Walch, 2015).

Magnetic field orientation relative to density structures may indicate their role in the ISM evolution (e.g., Soler and Hennebelle, 2017). Observations of plane-of-sky magnetic fields ($B_{\rm POS}$; e.g., Planck

Collaboration et al., 2016; Soler, 2019) show that they tend to be perpendicular to high-column-density structures ($N_H > 10^{21.7}$) and parallel to low-column-density ones. The relation between the transition from parallel to perpendicular alignment and gravitational collapse or Alfvén Mach number ($\mathcal{M}_A$) is being studied (e.g., Chen et al., 2016; Soler and Hennebelle, 2017; Soler et al., 2017; Pattle et al., 2021). 3D magnetic field measurements are necessary to understand this alignment (Girichidis, 2021, particularly since field lines may be inclined along the line of sight).

The magnetic field inclination angle with respect to the plane of the sky (γ) also complicates inferring $\mathcal{M}_A$ and mass-to-flux ratio (μ_ϕ), two key quantities in examining the role of magnetic fields in star formation. $\mathcal{M}_A$ and μ_ϕ quantify the cloud's magnetic energy relative to its kinetic/turbulent and gravitational energies, respectively (see Pattle et al., 2021, and references therein). Without estimating the 3D fields, a sub-Alfvénic cloud ($\mathcal{M}_A < 1$; with highly inclined ordered field lines) may be misinterpreted as a super-Alfvénic cloud ($\mathcal{M}_A > 1$ with tangled field lines dominated by the flow; Falceta-Gonçalves et al., 2008). Additionally, using field strengths based on a single component instead of 3D vectors may lead to incorrect estimates of μ_ϕ and the relationship between the cloud's magnetic field and gravitational energies (Crutcher et al., 2010; Mouschovias and Tassis, 2010; Clemens et al., 2016; Pillai et al., 2016).

Moreover, 3D magnetic field observations allow comparison of their morphologies to cloud-formation model predictions, enabling us to investigate ISM evolution and molecular-cloud formation. While observed magnetic field morphologies are consistent with some cloud-formation models (e.g., Inoue and Fukui, 2013; Inutsuka et al., 2015, 2016; Gómez et al., 2018; Inoue et al., 2018; Abe et al., 2021), observing the 3D magnetic fields of a large number of clouds is required to study their formation scenario and determine how magnetic fields influence the evolution of these clouds into filaments, cores, and, eventually, stars.

Despite the rise of recent techniques to observe interstellar magnetic fields (Clark et al., 2014; González-Casanova and Lazarian, 2017; Tahani et al., 2018; Lazarian and Yuen, 2018; Hu et al., 2019), probing the 3D fields remains exceedingly challenging. To infer the 3D fields, observations of both line-of-sight magnetic fields ($B_{\rm LOS}$) and $B_{\rm POS}$ are required. Common techniques for observing the interstellar magnetic fields (see Pattle et al., 2022, and references therein for details) include Zeeman splitting (Crutcher and Kemball, 2019), Faraday rotation (Brown et al., 2008), dust emission polarization (Draine, 2003), starlight (dust extinction) polarization (Voshchinnikov, 2012), and synchrotron emission (Beck, 2015). This mini-review focuses on *molecular clouds*[1] (a few to ~ 100 pc). For molecular clouds, Zeeman splitting and the Faraday-based technique of Tahani et al. (2018) provide $B_{\rm LOS}$, while dust emission and starlight polarization provide $B_{\rm POS}$. We present techniques for probing the 3D magnetic fields of molecular clouds in Section 2 and discuss their applications and future directions in Section 3.

2 3D MAGNETIC FIELDS

Several methods (e.g., Chen et al., 2019; Hu et al., 2021b,a; Tahani et al., 2019, 2022a,b; Hu and Lazarian, 2022) have examined the 3D magnetic fields of molecular clouds. Chen et al. (2019) and Hu and Lazarian (2022) use $B_{\rm POS}$ (dust polarization) observations and their polarization fraction (p) to recover the mean inclination of the ordered[2] magnetic fields of molecular clouds, whereas Tahani et al. (2022a,b, scales of a few to ~ 100 pc) incorporate $B_{\rm LOS}$ and $B_{\rm POS}$ observations along with Galactic magnetic field (GMF) models.

[1] A number of recent studies have examined the 3D magnetic fields of the diffuse ISM (e.g., Ferrière, 2016; Van Eck et al., 2017; Alves et al., 2018; Panopoulou et al., 2019; Clark and Hensley, 2019; Hensley et al., 2019).

[2] ordered: ignoring the random component due to turbulence or smaller-scale variations

Numerous observatories, including the James Clark Maxwell Telescope (JCMT; e.g., Eswaraiah et al., 2021; Ngoc et al., 2021; Hwang et al., 2021; Kwon et al., 2022), Planck Space Observatory (e.g., Planck Collaboration et al., 2016; Alina et al., 2019), Atacama Large Millimeter/sub-millimeter Array (ALMA; e.g., Pattle et al., 2021; Cortés et al., 2021), Sub-Millimeter Array (SMA; e.g., Zhang et al., 2014), and Stratospheric Observatory for Infrared Astronomy (SOFIA; e.g., Chuss et al., 2019) have observed $B_{\rm POS}$ of numerous star-forming regions. However, the number of $B_{\rm LOS}$ observations of molecular clouds are still limited. Although Zeeman splitting is a powerful technique for probing $B_{\rm LOS}$ and the most accurate method for determining field strengths, it requires lengthy observing runs, making it challenging to observe. The observing technique of Tahani et al. (2018) can be used to map $B_{\rm LOS}$ of numerous molecular clouds.

2.1 Line-of-sight magnetic fields

Tahani et al. (2018) developed a new technique to probe $B_{\rm LOS}$ associated with molecular clouds, using Faraday rotation. We provide a brief summary of the technique in this section.

2.1.1 Faraday rotation

Due to the lower abundance of electrons in molecular clouds (compared to ionized regions), it was previously believed that Faraday rotation[3] could not be used to investigate the magnetic fields of molecular clouds. Tahani et al. (2018) developed a technique to successfully determine $B_{\rm LOS}$ of molecular clouds using Faraday rotation measures (RM), while previous attempts (Reich et al., 2002; Wolleben and Reich, 2004) were unable to provide a map of $B_{\rm LOS}$ observations across the cloud.

2.1.2 Methodology and results

In this technique (Tahani et al., 2018), the non-cloud (background and foreground; Galactic) contribution to the RM ($\rm RM_{ref}$) is subtracted from the observed RM of extra-galactic point sources (radio galaxies or quasars) using an on-off approach. Numerous catalogs (e.g., Taylor et al., 2009) provide observed RM point sources. Following the determination of the the cloud's RMs, the electron column densities associated with each RM point are calculated using a chemical evolution code and extinction maps. Any chemical evolution code (e.g., one used by Gibson et al., 2009) and extinction map (e.g., Kainulainen et al., 2009), or even Hydrogen column density map (Lombardi et al., 2014; Zari et al., 2016), can be utilized. To find electron column densities, the cloud is divided into sub-layers aligned along the line of sight using extinction values and the chemical code. The electron column density in each sub-layer is obtained separately. Calculating the average $B_{\rm LOS}$ along the line of sight is made possible by adding the electron column density contributions of these sub-layers.

Tahani et al. (2018) mapped $B_{\rm LOS}$ of the Orion A, Orion B, California, and Perseus molecular clouds and found that their results were consistent with existing molecular Zeeman measurements. They found that the $B_{\rm LOS}$ direction of the Orion A (see left panel of Figure 1) and California clouds reverses from one side to the other (along the short axis of the cloud). Their Perseus results suggested a weak indication of this reversal. The $B_{\rm LOS}$ reversal across Orion A was previously observed via Zeeman splitting (Heiles, 1997), in the same directions as Tahani et al. (2018).

Identifying a) direction and b) strength are the two components of $B_{\rm LOS}$ determination in this technique. The direction uncertainty arises from uncertainties in a) observed RM values and b) $\rm RM_{ref}$. The strength uncertainty arises from assumptions of a) constant $B_{\rm LOS}$ along the line of sight, b) symmetry of the cloud

[3] A number of review articles discuss Faraday rotation and its observations (e.g., Brown et al., 2008; Noutsos, 2012; Han, 2017).

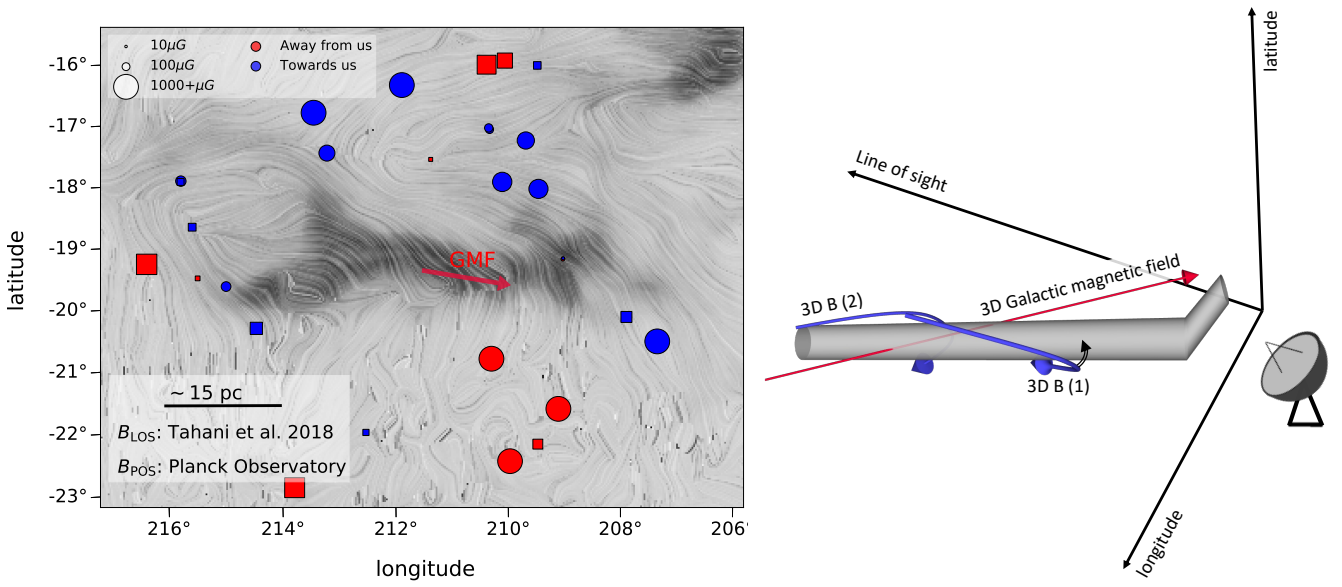

Figure 1. 3D magnetic field of the Orion A cloud. **Left panel:** The grayscale image illustrates the hydrogen column density map of Orion A (Lombardi et al., 2014). The circle and square markers represent $B_{\rm LOS}$, with the square indicating non-detection points (with high uncertainties that may cause a change in $B_{\rm LOS}$ direction) and blue (red) representing pointing toward (away from) us. The drapery lines represent the $B_{\rm POS}$ observed by the Planck Space Observatory. The red vector depicts the modeled Galactic Magnetic field projected onto the plane of the sky. The same $B_{\rm LOS}$ reversal throughout the cloud was previously detected using Zeeman measurements (Heiles, 1997, see their Figure 15). We note that in Zeeman measurements, the negative sign indicates magnetic field directed toward us, while in RM studies, it indicates magnetic field directed away from us. **Right panel:** From our vantage point, the inferred 3D ordered magnetic field of Orion A is semi-convex. The red vector, bent gray cylinder, and blue vectors represent the modeled GMF, cloud, and 3D magnetic field of the cloud, respectively. Without identifying the inclination angle of the cloud, rotations of up to 50° along the black arrow may be possible, resulting in both B(1) and B(2) (see Section 2 of Tahani et al., 2022a).

along the line of sight, c) parameters taken to estimate electron densities (cloud's initial temperature and density and Ultra-Violet and cosmic ionization rates), and d) extinction maps.

2.2 Plane of sky magnetic fields

Dust emission polarization has been successfully applied to molecular clouds (e.g., Planck Collaboration et al., 2016; Pattle and Fissel, 2019). The technique is based on the alignment of the long axis of amorphous dust grains (e.g., Draine, 2009) perpendicular to magnetic fields, resulting in linear polarization and explained by radiative torque alignment (RAT; Draine and Weingartner, 1997; Lazarian, 2007; Lazarian and Hoang, 2007; Andersson et al., 2015; Hoang and Lazarian, 2016). The Davis-Chandrasekhar-Fermi technique (DCF; Davis and Greenstein, 1951; Chandrasekhar and Fermi, 1953) or its subsequent modified versions (e.g., Ostriker et al., 2001; Houde et al., 2009; Skalidis and Tassis, 2021; Skalidis et al., 2021a) are utilized to estimate $B_{\rm POS}$ strengths (see Pattle and Fissel, 2019; Pattle et al., 2022, for more information and the technique's limitations).

2.3 Reconstructing the mean 3D magnetic fields of molecular clouds

Using $B_{\rm LOS}$ observations, Tahani et al. (2019, 2022a,b) studied the 3D magnetic field morphologies of the Orion A and Perseus molecular clouds. Tahani et al. (2019) constrained models of the ordered, cloud-scale magnetic field, using $B_{\rm POS}$ angles and $B_{\rm LOS}$ estimates, whereas Tahani et al. (2022a,b) inferred

cloud-scale magnetic field vectors in 3D[4], given a set of model assumptions. We discuss these techniques in this section.

2.3.1 Analytical models of the ordered magnetic field within clouds and comparison to synthetic observations

Tahani et al. (2019) constructed models that could explain the observed $B_{\rm LOS}$ reversal discussed in Section 2.1.2, obtained synthetic observations from the models, and compared these synthetic observations with $B_{\rm LOS}$ (direction and strengths) and $B_{\rm POS}$ (angle and strength; using Planck[5]) estimates of Orion A. They concluded that an arc-shaped morphology (see right panel of Figure 1) is the most probable magnetic morphology for Orion A, based on Monte-Carlo analysis, chi-square probability values, and examination of a range of systematic biases between $B_{\rm LOS}$ and $B_{\rm POS}$ observations. In the arc-shaped morphology, field lines bend around the filamentary cloud in response to environmental interaction (first proposed by Heiles, 1997), enabling mass to flow along the field lines and accumulate on the cloud (Inoue et al., 2018).

2.3.2 Using Galactic magnetic field models to reconstruct the cloud-scale ordered magnetic field 3D vector

Tahani et al. (2022a,b) reconstructed the cloud-scale, ordered magnetic field vectors of the Orion A and Perseus clouds in 3D. Using $B_{\rm LOS}$ and $B_{\rm POS}$ observations, along with large-scale GMF models (Jansson and Farrar, 2012a,b), they inferred the approximate orientation and direction[6] of the 3D ordered magnetic field of these clouds (including their $B_{\rm POS}$ *direction*). Although the $B_{\rm POS}$ *orientation* of numerous molecular clouds had been observed previously, their $B_{\rm POS}$ *direction* remained undetermined even in the 3D study by Tahani et al. (2019).

Moreover, by estimating $\mathcal{M}_A$ values and/or comparing estimates of initial magnetic field vectors (using GMF models) with $B_{\rm POS}$ maps, Tahani et al. (2022a,b) suggest that the magnetic fields of the Orion A and Perseus clouds retain a memory of the Galactic magnetic fields. Although some studies (e.g., Stephens et al., 2011) have suggested that the magnetic fields of molecular clouds are dissociated from larger Galactic scales, others (e.g., Han and Zhang, 2007) have concluded that they largely retain the large-scale Galactic magnetic fields.

We note that this technique relies on correctly identifying the ordered GMF vector at the cloud location. This vector provides an approximation of the initial magnetic fields prior to the cloud's evolution (allowing us to ignore the GMF random component caused by cloud-scale turbulence). Since GMF models vary (Jaffe, 2019), this technique is applied to clouds in a region of the Galaxy (pointing anti-Galactic and nearby) where there is less disagreement between the GMF models. For example, all models in Figure 2 from Jaffe (2019), except panel h (Fauvet et al., 2011), generate similar ordered GMF vectors at the locations of the Orion A and Perseus clouds. Moreover, the limited number of $B_{\rm LOS}$ observations per cloud and the use of two tracers (dust emission and a Faraday-based technique) may increase the technique's uncertainties. Upcoming observations are required to advance these studies (see Section 3).

[4] approximate 3D morphology at scales of a few to 100 pc (ignoring turbulence and smaller-scale variations)

[5] `http://www.esa.int/Planck`

[6] In this mini-review we distinguish between the terms *direction* and *orientation*. Knowing the direction reveals orientation, but not the other way around. For example, the direction of $B_{\rm LOS}$ indicates either away from us or toward us, whereas the orientation of $B_{\rm LOS}$ indicates only that the line is parallel to the line of sight without specifying its direction. Similarly for $B_{\rm POS}$, direction refers to the complete 2D vector, while orientation refers only to the line without specifying the vector's endpoint.

2.4 Inclination angle: statistical studies of polarization fraction

The 3D morphologies identified by Tahani et al. (2022a,b) can be improved by inferring γ at various points across the cloud and combining their method with studies that estimate γ (e.g., Chen et al., 2019; Sullivan et al., 2021; Hu et al., 2021a, 2022; Hu and Lazarian, 2022). In recent years, γ has been inferred in molecular clouds (e.g., Sullivan et al., 2021) and diffuse ISM[7] (e.g., Hensley et al., 2019), using the dependence of p and polarization angle dispersion ($\mathcal{S}$) on γ (e.g., Falceta-Gonçalves et al., 2008; Hensley et al., 2019), under the assumption of homogeneous grain alignment efficiency.

King et al. (2018) compared the p and $\mathcal{S}$ values of the Vela C cloud with their 3D, ideal magnetohydrodynamics (MHD) colliding flow simulations. The simulations were performed using the ATHENA code (Stone et al., 2008) and included gravity. Statistical comparisons (using relative orientation of column density and magnetic fields, average γ, and $\mathcal{S}$) between these simulations and observations explored the effect of γ on p and $\mathcal{S}$ and were made possible by the high resolution and sensitivity of the Balloon-borne Large Aperture Sub-millimeter Telescope for Polarimetry (BLASTPol) observations of the Vela C (Fissel et al., 2016) cloud. These comparisons indicated that the Vela C observations and its high polarization angle dispersion were consistent with simulations of magnetic fields with high inclination angles. However, due to the degeneracy between disorder caused by turbulence and disorder caused by a large inclination angle (the field disorder seen in the plane of the sky), they were unable to infer a γ value for the Vela C cloud.

Chen et al. (2019) extended the study of King et al. (2018) and determined γ for the Vela C cloud, assuming a small total $\mathcal{S}$ (applicable only to sub-Alfvénic regions). Using a statistical examination of the p values of the cloud and the maximum polarization fraction (associated with zero inclination), they calculated γ. They found an average γ value of $\sim 60^\circ$ for the Vela C cloud, with an estimated accuracy of $\leq 10^\circ - 30^\circ$. Subsequently, Sullivan et al. (2021) analyzed the 3D magnetic field properties of nearby molecular clouds[8] and estimated their cloud-averaged γ values. This technique can be used to examine the relative alignment of magnetic field lines and the orientation of filamentary dense gas in 3D (Fissel et al., 2019).

The technique's inherent uncertainty is dominated by the following assumptions: a) presence of a location within the cloud with zero γ, corresponding to the observed maximum p; b) homogeneous grain alignment efficiency across the cloud[9]; c) neglecting depolarization effects along the line of sight; d) assuming uni-directional magnetic fields along the line of sight; and e) ordered field line, which was addressed by Hu and Lazarian (2022). Hu and Lazarian (2022) augmented the technique of Chen et al. (2019) by incorporating magnetic field fluctuations and dispersion (making the technique applicable to trans- and super-Alfvénic regions as well). They modified the equations of Chen et al. (2019) on the assumption that field fluctuations are perpendicular to the mean field. Additionally, we note that these studies still require both $B_{\rm LOS}$ and $B_{\rm POS}$ *directions* to infer 3D vectors (see Figure 2).

2.5 Other approaches

While this mini-review focuses on the techniques discussed in Sections 2.3 and 2.4 and their combination for recovering the 3D magnetic fields of *molecular clouds*, we note that other more theory-based techniques can also be used in clouds (e.g., Yan and Lazarian, 2005; Tritsis and Tassis, 2018; Hu et al., 2021a;

[7] where dust emission intensity per atomic hydrogen column density may also be used to infer γ (Hensley et al., 2019).

[8] The Aquila Rift, Cepheus, Chameleon-Musca, Corona Australis, Lupus, Ophiuchus, Perseus, Taurus, and Vela C clouds

[9] King et al. (2019) suggest that the correlation between $\mathcal{S}$ and γ used in the Chen et al. (2019) technique is maintained, even in the absence of homogeneous grain alignment efficiency, assuming a power-law relation between grain alignment efficiency and local gas density.

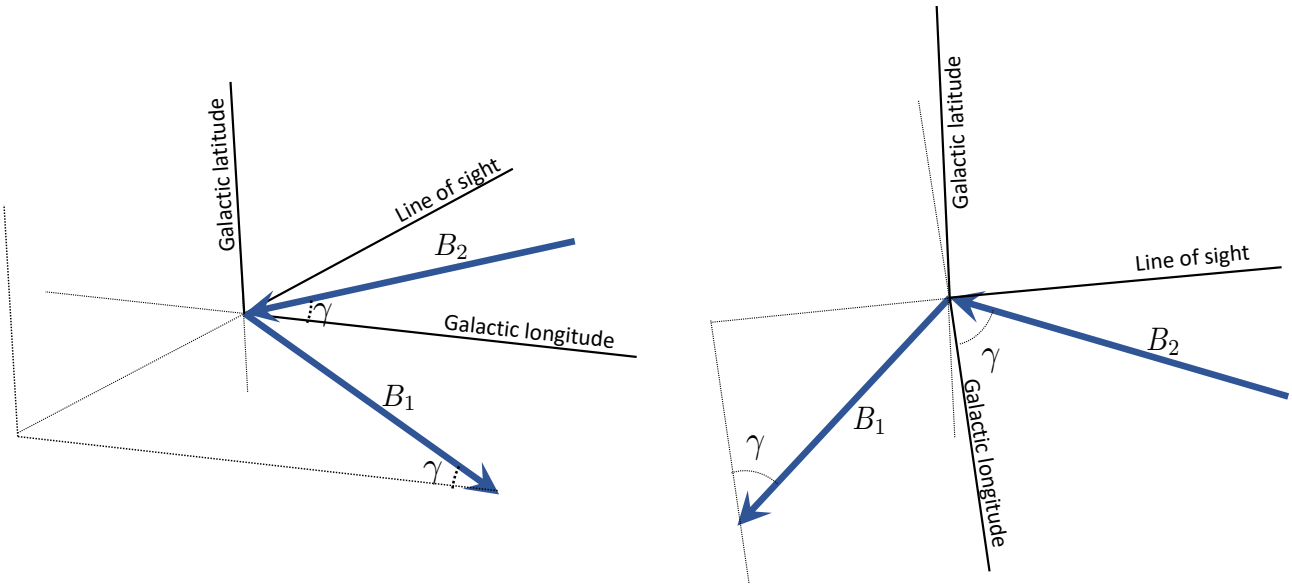

Figure 2. $B_{\rm POS}$ direction required for 3D field determination. The 3D magnetic field vectors B_1 and B_2 have the same inclination angle (γ), run parallel to the Galactic longitude axis when projected onto the plane of the sky, and point toward us when projected along the line of sight. However, due to the difference in their $B_{\rm POS}$ directions, they are two distinct 3D vectors. Since the projections of these two vectors onto the plane of the sky are parallel to the longitude axis, their inclination angle with respect to the plane of the sky is the angle between the 3D vector and the longitude axis. The left and right panels display two different viewing angles. Distinguishing between these two vectors is particularly important in studies of relative alignment of field lines and clouds, as a cloud aligned with B_1 may be approximately perpendicular to B_2 depending on the value of γ.

Skalidis et al., 2021b) or within its high density regions (i.e., clumps or cores Houde et al., 2000a; Kandori et al., 2017, 2020a,b,c). We briefly discuss these techniques here, excluding those applicable only to core scales (e.g., Kandori et al., 2017, 2020a,b,c).

2.5.1 Ion-to-neutral line-width

Houde et al. (2000a,b, 2002, 2004) proposed a method for measuring γ based on the ion-to-neutral line-width ratios. Their observations showed that, in the presence of strong magnetic fields, the line-width of ions is narrower than that of coexisting neutrals. They suggest that when the field lines are perpendicular to the line of sight, the difference in line-widths should be the greatest, enabling them to infer γ. Some studies found supporting (Li and Houde, 2008; Hezareh et al., 2010; Houde, 2011; Tang et al., 2018) or inconsistent (Pineda et al., 2021) observational evidence.

2.5.2 Atomic alignment

The atomic alignment (or ground state alignment) technique (Yan and Lazarian, 2005, 2006, 2007, 2012; Yan et al., 2019) relies on the alignment of the angular momentum of atoms in their ground state with the photons' angular momentum from background anisotropic radiation, followed by their realignment with external magnetic fields. For best outcomes, absorption lines are used. Calculating the degree of alignment with magnetic field lines, Yan and Lazarian (2007) obtained the Stokes parameters of absorbed radiation and compared them with observations to infer γ and the 3D field lines. This method is most applicable to diffuse ISM (Yan and Lazarian, 2012), but may also be applied to molecular clouds and their envelopes.

2.5.3 Young stellar objects and position-position-velocity space techniques

Based on the observable anisotropy of turbulence eddies in the presence of magnetic fields, Hu et al. (2021b) estimate magnetic fields using structure function analysis (SFA). They demonstrate that for sub-Alfvénic regions, the ratio of perpendicular to parallel[10] velocity fluctuations has a power-law relation with $\mathcal{M}_A$, enabling determination of 3D field strengths. Hu et al. (2021a) extended the SFA analysis of Hu et al. (2021b) to infer 3D fields by incorporating Gaia observations of young stellar objects (for estimating 3D velocity fluctuations; assuming they inherit the velocity of their parent cloud).

2.6 Potential insights from 3D field mapping

This section briefly discusses the potential takeaways from the aforementioned 3D studies. Assuming a GMF model and given $B_{\rm LOS}$ and $B_{\rm POS}$ observations, Tahani et al. (2022b,a) inferred the 3D ordered magnetic field vectors of two molecular clouds. Including γ can enhance these studies. Inferring the 3D magnetic fields of numerous molecular clouds will enable us to compare them with models and numerical simulations to constrain cloud formation models (see Hennebelle and Inutsuka, 2019, and references therein), 3D structure and evolution of the ISM (e.g., Hacar et al., 2022), 3D GMF models (e.g., Jaffe, 2019), and the role of magnetic fields in cloud evolution (e.g., Fiege and Pudritz, 2000a).

For example, Tahani et al. (2022b) employed velocity information of the Perseus cloud along with GMF models to predict the cloud-averaged ordered line-of-sight and 3D magnetic field of this cloud based on the model of Inutsuka et al. (2015)[11] and found the predictions to be consistent with their inferred 3D field and $B_{\rm LOS}$ data. The cloud-formation model of Inutsuka et al. (2015) requires multiple compressions caused by expanding interstellar bubbles to form filamentary molecular clouds. Using dynamics and bubble observations of the Orion A and Perseus clouds, Tahani et al. (2022a,b) proposed similar formation scenarios for their 3D fields: the field lines should have been initially bent on a large scale by recurrent supernovae shocks. This bending of field lines by bubbles has been detected in numerical simulations (Kim and Ostriker, 2015) and large- and small-scale observations (Soler et al., 2018; Bracco et al., 2020; Arzoumanian et al., 2021). Subsequently, interaction with a secondary bubble may have pushed the HI gas surrounding the clouds, causing a sharp field line bending (arc-shaped field) associated with the molecular cloud.

Velocity profile observations may also shed light on the formation process or 3D structure of clouds (e.g., Tritsis and Tassis, 2018; Arzoumanian et al., 2018; Bonne et al., 2020). Position-position-velocity space studies of these clouds can improve the precision and accuracy of these 3D fields to explore their consistency with theoretical and numerical models (e.g., Clark et al., 2014, 2015; González-Casanova and Lazarian, 2017; Clark, 2018; Clark and Hensley, 2019; Hu et al., 2019, 2020, 2021a,b, 2022).

3 DISCUSSION

Observing the 3D magnetic fields of molecular clouds and their substructures is essential for understanding their formation mechanism and the role magnetic fields play in star formation. Observations of $B_{\rm LOS}$ and $B_{\rm POS}$ are necessary but insufficient for determining the 3D fields. While $B_{\rm LOS}$ observing techniques provide both the strength and direction of this component, $B_{\rm POS}$ observing techniques provide only the orientation and strength of this component, but not its direction. Knowing the strengths and complete directions of $B_{\rm LOS}$ and $B_{\rm POS}$ enables us to infer the ordered, line-of-sight-averaged 3D field vectors.

[10] relative to the magnetic field

[11] also see simulations by Inoue et al. (2018)

However, due to systematic biases between the techniques for determining field strengths, additional observations, such as observing the magnetic field inclination angles are required. The $B_{\rm LOS}$ strength and direction, γ, and $B_{\rm POS}$ orientation (without its direction) do not fully infer the 3D fields, as they can lead to two different vectors depicted in Figure 2. Other techniques such as the use of GMF models (Tahani et al., 2022a,b) can help resolve this issue.

The studies of $B_{\rm LOS}$, $B_{\rm POS}$, γ, and GMF could enable us to infer the 3D ordered magnetic fields of molecular clouds with improved precision. Upcoming observations will 1) enhance the precision and accuracy of the inferred 3D magnetic field of each cloud, 2) result in 3D magnetic field maps of more regions, and 3) produce more accurate GMF models, thereby enhancing the technique's underlying assumptions.

The forthcoming Zeeman measurements (Robishaw et al., 2015, for the most accurate determination of field strengths) and Faraday rotation measure catalogs by the Square Kilometer Array (SKA) project (Heald et al., 2020) or the Australian Square Kilometer Array Pathfinder (ASKAP), such as the Polarisation Sky Survey of the Universe's Magnetism (POSSUM) rotation measure catalog (Gaensler et al., 2010), will provide the $B_{\rm LOS}$ of numerous molecular clouds with lower uncertainties and greater source density than previous catalogs (e.g., Taylor et al., 2009). These observations will increase the number of $B_{\rm LOS}$ detections per molecular cloud by a factor of ~ 10. These $B_{\rm LOS}$ maps and future $B_{\rm POS}$ observations, such as those by the Fred Young Sub-millimeter Telescope (FYST; CCAT-Prime collaboration et al., 2021), will enable 3D magnetic field maps of many molecular clouds.

Finally, starlight polarization observations (e.g., Pereyra and Magalhães, 2007) combined with Gaia-observed parallax distances allow us to differentiate between, and separate, various cloud components along the line of sight (e.g., Doi et al., 2021). This is made possible by existing and upcoming starlight polarization observations, including the Galactic Plane Infrared Polarization Survey (GPIPS; Clemens et al., 2020) and the upcoming optical polarimetry survey with the Polar-Areas Stellar Imaging Polarization High Accuracy Experiment (PASIPHAE; Tassis et al., 2018).

ACKNOWLEDGMENTS

We appreciate the referees' insightful, thorough, and diligent comments. We thank Huirong Yan for helpful conversation about atomic alignment. Figure 1 employs a function written by Susan Clark and later modified by Jennifer Glover (Tahani et al., 2022a) to perform line integration convolution. Quillbot was utilized for editing purposes. MT was hired by the National Research Council Canada. MT is supported by the Banting Fellowship (Natural Sciences and Engineering Research Council Canada) hosted at Stanford University and the Kavli Institute for Particle Astrophysics and Cosmology (KIPAC) Fellowship.

REFERENCES

Abe, D., Inoue, T., Inutsuka, S.-i., and Matsumoto, T. (2021). Classification of Filament Formation Mechanisms in Magnetized Molecular Clouds. *ApJ* 916, 83. doi:10.3847/1538-4357/ac07a1

Alina, D., Ristorcelli, I., Montier, L., Abdikamalov, E., Juvela, M., Ferrière, K., et al. (2019). Statistical analysis of the interplay between interstellar magnetic fields and filaments hosting Planck Galactic cold clumps. *MNRAS* 485, 2825–2843. doi:10.1093/mnras/stz508

Alves, M. I. R., Boulanger, F., Ferrière, K., and Montier, L. (2018). The Local Bubble: a magnetic veil to our Galaxy. *A&A* 611, L5. doi:10.1051/0004-6361/201832637

Andersson, B.-G., Lazarian, A., and Vaillancourt, J. E. (2015). Interstellar Dust Grain Alignment. *ARA&A* 53, 501–539. doi:10.1146/annurev-astro-082214-122414

Arzoumanian, D., Furuya, R. S., Hasegawa, T., Tahani, M., Sadavoy, S., Hull, C. L. H., et al. (2021). Dust polarized emission observations of NGC 6334. BISTRO reveals the details of the complex but organized magnetic field structure of the high-mass star-forming hub-filament network. *A&A* 647, A78. doi:10.1051/0004-6361/202038624

Arzoumanian, D., Shimajiri, Y., Inutsuka, S.-i., Inoue, T., and Tachihara, K. (2018). Molecular filament formation and filament-cloud interaction: Hints from Nobeyama 45 m telescope observations. *PASJ* 70, 96. doi:10.1093/pasj/psy095

Beck, R. (2015). Magnetic fields in spiral galaxies. *A&A Rev.* 24, 4. doi:10.1007/s00159-015-0084-4

Bialy, S., Zucker, C., Goodman, A., Foley, M. M., Alves, J., Semenov, V. A., et al. (2021). The Per-Tau Shell: A Giant Star-forming Spherical Shell Revealed by 3D Dust Observations. *ApJ* 919, L5. doi:10.3847/2041-8213/ac1f95

Bonne, L., Bontemps, S., Schneider, N., Clarke, S. D., Arzoumanian, D., Fukui, Y., et al. (2020). Formation of the Musca filament: evidence for asymmetries in the accretion flow due to a cloud-cloud collision. *A&A* 644, A27. doi:10.1051/0004-6361/202038281

Bracco, A., Bresnahan, D., Palmeirim, P., Arzoumanian, D., André, P., Ward-Thompson, D., et al. (2020). Compressed magnetized shells of atomic gas and the formation of the Corona Australis molecular cloud. *A&A* 644, A5. doi:10.1051/0004-6361/202039282

Brown, J. C., Stil, J. M., and Landecker, T. L. (2008). Visualizing the Invisible using Polarisation Observations. *Physics in Canada* 64

CCAT-Prime collaboration, Aravena, M., Austermann, J. E., Basu, K., Battaglia, N., Beringue, B., et al. (2021). CCAT-prime Collaboration: Science Goals and Forecasts with Prime-Cam on the Fred Young Submillimeter Telescope. *arXiv e-prints* , arXiv:2107.10364

Chandrasekhar, S. and Fermi, E. (1953). Magnetic Fields in Spiral Arms. *ApJ* 118, 113. doi:10.1086/145731

Chen, C.-Y., King, P. K., and Li, Z.-Y. (2016). Change of Magnetic Field-gas Alignment at the Gravity-driven Alfvénic Transition in Molecular Clouds: Implications for Dust Polarization Observations. *ApJ* 829, 84. doi:10.3847/0004-637X/829/2/84

Chen, C.-Y., King, P. K., Li, Z.-Y., Fissel, L. M., and Mazzei, R. R. (2019). A new method to trace three-dimensional magnetic field structure within molecular clouds using dust polarization. *MNRAS* 485, 3499–3513. doi:10.1093/mnras/stz618

Chuss, D. T., Andersson, B. G., Bally, J., Dotson, J. L., Dowell, C. D., Guerra, J. A., et al. (2019). HAWC+/SOFIA Multiwavelength Polarimetric Observations of OMC-1. *ApJ* 872, 187. doi:10.3847/1538-4357/aafd37

Clark, S. E. (2018). A New Probe of Line-of-sight Magnetic Field Tangling. *ApJ* 857, L10. doi:10.3847/2041-8213/aabb54

Clark, S. E. and Hensley, B. S. (2019). Mapping the Magnetic Interstellar Medium in Three Dimensions over the Full Sky with Neutral Hydrogen. *ApJ* 887, 136. doi:10.3847/1538-4357/ab5803

Clark, S. E., Hill, J. C., Peek, J. E. G., Putman, M. E., and Babler, B. L. (2015). Neutral Hydrogen Structures Trace Dust Polarization Angle: Implications for Cosmic Microwave Background Foregrounds. *Phys. Rev. Lett.* 115, 241302. doi:10.1103/PhysRevLett.115.241302

Clark, S. E., Peek, J. E. G., and Putman, M. E. (2014). Magnetically Aligned H I Fibers and the Rolling Hough Transform. *ApJ* 789, 82. doi:10.1088/0004-637X/789/1/82

Clemens, D. P., Cashman, L. R., Cerny, C., El-Batal, A. M., Jameson, K. E., Marchwinski, R., et al. (2020). The Galactic Plane Infrared Polarization Survey (GPIPS): Data Release 4. *ApJS* 249, 23. doi:10.3847/1538-4365/ab9f30

Clemens, D. P., Tassis, K., and Goldsmith, P. F. (2016). The Magnetic Field of L1544. I. Near-infrared Polarimetry and the Non-uniform Envelope. *ApJ* 833, 176. doi:10.3847/1538-4357/833/2/176

Cortés, P. C., Sanhueza, P., Houde, M., Martín, S., Hull, C. L. H., Girart, J. M., et al. (2021). Magnetic Fields in Massive Star-forming Regions (MagMaR). II. Tomography through Dust and Molecular Line Polarization in NGC 6334I(N). *ApJ* 923, 204. doi:10.3847/1538-4357/ac28a1

Crutcher, R. M. and Kemball, A. J. (2019). Review of Zeeman Effect Observations of Regions of Star Formation K Zeeman Effect, Magnetic Fields, Star formation, Masers, Molecular clouds. *Frontiers in Astronomy and Space Sciences* 6, 66. doi:10.3389/fspas.2019.00066

Crutcher, R. M., Wandelt, B., Heiles, C., Falgarone, E., and Troland, T. H. (2010). Magnetic Fields in Interstellar Clouds from Zeeman Observations: Inference of Total Field Strengths by Bayesian Analysis. *ApJ* 725, 466–479. doi:10.1088/0004-637X/725/1/466

Davis, L. J. and Greenstein, J. L. (1951). The Polarization of Starlight by Aligned Dust Grains. *ApJ* 114, 206. doi:10.1086/145464

Doi, Y., Hasegawa, T., Bastien, P., Tahani, M., Arzoumanian, D., Coudé, S., et al. (2021). Two-component Magnetic Field along the Line of Sight to the Perseus Molecular Cloud: Contribution of the Foreground Taurus Molecular Cloud. *ApJ* 914, 122. doi:10.3847/1538-4357/abfcc5

Draine, B. T. (2003). Interstellar Dust Grains. *ARA&A* 41, 241–289. doi:10.1146/annurev.astro.41.011802.094840

Draine, B. T. (2009). Interstellar Dust Models and Evolutionary Implications. In *Cosmic Dust - Near and Far*, eds. T. Henning, E. Grün, and J. Steinacker. vol. 414 of *Astronomical Society of the Pacific Conference Series*, 453

Draine, B. T. and Weingartner, J. C. (1997). Radiative Torques on Interstellar Grains. II. Grain Alignment. *ApJ* 480, 633–646. doi:10.1086/304008

Eswaraiah, C., Li, D., Furuya, R. S., Hasegawa, T., Ward-Thompson, D., Qiu, K., et al. (2021). The JCMT BISTRO Survey: Revealing the Diverse Magnetic Field Morphologies in Taurus Dense Cores with Sensitive Submillimeter Polarimetry. *ApJ* 912, L27. doi:10.3847/2041-8213/abeb1c

Falceta-Gonçalves, D., Lazarian, A., and Kowal, G. (2008). Studies of Regular and Random Magnetic Fields in the ISM: Statistics of Polarization Vectors and the Chandrasekhar-Fermi Technique. *ApJ* 679, 537–551. doi:10.1086/587479

Fauvet, L., Macías-Pérez, J. F., Aumont, J., Désert, F. X., Jaffe, T. R., Banday, A. J., et al. (2011). Joint 3D modelling of the polarized Galactic synchrotron and thermal dust foreground diffuse emission. *A&A* 526, A145. doi:10.1051/0004-6361/201014492

Ferrière, K. (2016). Faraday tomography: a new, three-dimensional probe of the interstellar magnetic field. In *Journal of Physics Conference Series*. vol. 767 of *Journal of Physics Conference Series*, 012006. doi:10.1088/1742-6596/767/1/012006

Fiege, J. D. and Pudritz, R. E. (2000a). Helical fields and filamentary molecular clouds - I. *MNRAS* 311, 85–104. doi:10.1046/j.1365-8711.2000.03066.x

Fiege, J. D. and Pudritz, R. E. (2000b). Helical fields and filamentary molecular clouds - II. Axisymmetric stability and fragmentation. *MNRAS* 311, 105–119. doi:10.1046/j.1365-8711.2000.03067.x

Fissel, L. M., Ade, P. A. R., Angilè, F. E., Ashton, P., Benton, S. J., Chen, C.-Y., et al. (2019). Relative Alignment between the Magnetic Field and Molecular Gas Structure in the Vela C Giant Molecular Cloud Using Low- and High-density Tracers. *ApJ* 878, 110. doi:10.3847/1538-4357/ab1eb0

Fissel, L. M., Ade, P. A. R., Angilè, F. E., Ashton, P., Benton, S. J., Devlin, M. J., et al. (2016). Balloon-Borne Submillimeter Polarimetry of the Vela C Molecular Cloud: Systematic Dependence of Polarization Fraction on Column Density and Local Polarization-Angle Dispersion. *ApJ* 824, 134. doi:10.3847/0004-637X/824/2/134

Gaensler, B. M., Landecker, T. L., Taylor, A. R., and POSSUM Collaboration (2010). Survey Science with ASKAP: Polarization Sky Survey of the Universe's Magnetism (POSSUM). In *American Astronomical Society Meeting Abstracts #215*. vol. 215 of *American Astronomical Society Meeting Abstracts*, 470.13

Gaia Collaboration, Prusti, T., de Bruijne, J. H. J., Brown, A. G. A., Vallenari, A., Babusiaux, C., et al. (2016). The Gaia mission. *A&A* 595, A1. doi:10.1051/0004-6361/201629272

Gibson, D., Plume, R., Bergin, E., Ragan, S., and Evans, N. (2009). Molecular Line Observations of Infrared Dark Clouds. II. Physical Conditions. *ApJ* 705, 123–134. doi:10.1088/0004-637X/705/1/123

Girichidis, P. (2021). Alignment of the magnetic field in star-forming regions and why it might be difficult to observe. *MNRAS* 507, 5641–5657. doi:10.1093/mnras/stab2157

Gómez, G. C., Vázquez-Semadeni, E., and Zamora-Avilés, M. (2018). The magnetic field structure in molecular cloud filaments. *MNRAS* 480, 2939–2944. doi:10.1093/mnras/sty2018

González-Casanova, D. F. and Lazarian, A. (2017). Velocity Gradients as a Tracer for Magnetic Fields. *ApJ* 835, 41. doi:10.3847/1538-4357/835/1/41

Großschedl, J. E., Alves, J., Meingast, S., Ackerl, C., Ascenso, J., Bouy, H., et al. (2018). 3D shape of Orion A from Gaia DR2. *A&A* 619, A106. doi:10.1051/0004-6361/201833901

Hacar, A., Clark, S., Heitsch, F., Kainulainen, J., Panopoulou, G., Seifried, D., et al. (2022). Initial Conditions for Star Formation: A Physical Description of the Filamentary ISM. *arXiv e-prints* , arXiv:2203.09562

Han, J. L. (2017). Observing Interstellar and Intergalactic Magnetic Fields. *ARA&A* 55, 111–157. doi:10.1146/annurev-astro-091916-055221

Han, J. L. and Zhang, J. S. (2007). The Galactic distribution of magnetic fields in molecular clouds and HII regions. *A&A* 464, 609–614. doi:10.1051/0004-6361:20065801

Haverkorn, M. (2015). Magnetic Fields in the Milky Way. In *Magnetic Fields in Diffuse Media*, eds. A. Lazarian, E. M. de Gouveia Dal Pino, and C. Melioli. vol. 407 of *Astrophysics and Space Science Library*, 483. doi:10.1007/978-3-662-44625-6_17

Heald, G., Mao, S., Vacca, V., Akahori, T., Damas-Segovia, A., Gaensler, B., et al. (2020). Magnetism Science with the Square Kilometre Array. *Galaxies* 8, 53. doi:10.3390/galaxies8030053

Heiles, C. (1997). A Holistic View of the Magnetic Field in the Eridanus/Orion Region. *ApJS* 111, 245–288. doi:10.1086/313010

Hennebelle, P. and Inutsuka, S.-i. (2019). The role of magnetic field in molecular cloud formation and evolution. *arXiv e-prints* , arXiv:1902.00798

Hensley, B. S., Zhang, C., and Bock, J. J. (2019). An Imprint of the Galactic Magnetic Field in the Diffuse Unpolarized Dust Emission. *ApJ* 887, 159. doi:10.3847/1538-4357/ab5183

Hezareh, T., Houde, M., McCoey, C., and Li, H.-b. (2010). Observational Determination of the Turbulent Ambipolar Diffusion Scale and Magnetic Field Strength in Molecular Clouds. *ApJ* 720, 603–607. doi:10.1088/0004-637X/720/1/603

Hoang, T. and Lazarian, A. (2016). A Unified Model of Grain Alignment: Radiative Alignment of Interstellar Grains with Magnetic Inclusions. *ApJ* 831, 159. doi:10.3847/0004-637X/831/2/159

Houde, M. (2011). Magnetic Fields in Three Dimensions. In *Astronomical Polarimetry 2008: Science from Small to Large Telescopes*, eds. P. Bastien, N. Manset, D. P. Clemens, and N. St-Louis. vol. 449 of *Astronomical Society of the Pacific Conference Series*, 213

Houde, M., Bastien, P., Dotson, J. L., Dowell, C. D., Hildebrand, R. H., Peng, R., et al. (2002). On the Measurement of the Magnitude and Orientation of the Magnetic Field in Molecular Clouds. *ApJ* 569, 803–814. doi:10.1086/339356

Houde, M., Bastien, P., Peng, R., Phillips, T. G., and Yoshida, H. (2000a). Probing the Magnetic Field with Molecular Ion Spectra. *ApJ* 536, 857–864. doi:10.1086/308980

Houde, M., Peng, R., Phillips, T. G., Bastien, P., and Yoshida, H. (2000b). Probing the Magnetic Field with Molecular Ion Spectra. II. *ApJ* 537, 245–254. doi:10.1086/309035

Houde, M., Peng, R., Yoshida, H., Hildebrand, R. H., Phillips, T. G., Dowell, C. D., et al. (2004). The Measurement of the Orientation of the Magnetic Field in Molecular Clouds. *Ap&SS* 292, 127–134. doi:10.1023/B:ASTR.0000045008.39439.5b

Houde, M., Vaillancourt, J. E., Hildebrand, R. H., Chitsazzadeh, S., and Kirby, L. (2009). Dispersion of Magnetic Fields in Molecular Clouds. II. *ApJ* 706, 1504–1516. doi:10.1088/0004-637X/706/2/1504

Hu, Y. and Lazarian, A. (2022). Probing Three-Dimensional Magnetic Fields: I – Polarized Dust Emission. *arXiv e-prints* , arXiv:2203.09745

Hu, Y., Lazarian, A., and Wang, Q. D. (2022). Decomposing Magnetic Fields in Three Dimensions over the Central Molecular Zone. *MNRAS* doi:10.1093/mnras/stac1060

Hu, Y., Lazarian, A., and Xu, S. (2021a). Anisotropic Turbulence in Position-Position-Velocity Space: Probing Three-dimensional Magnetic Fields. *ApJ* 915, 67. doi:10.3847/1538-4357/ac00ab

Hu, Y., Lazarian, A., and Yuen, K. H. (2020). Velocity Gradient in the Presence of Self-gravity: Identifying Gravity-induced Inflow and Determining Collapsing Stage. *ApJ* 897, 123. doi:10.3847/1538-4357/ab9948

Hu, Y., Xu, S., and Lazarian, A. (2021b). Anisotropies in Compressible MHD Turbulence: Probing Magnetic Fields and Measuring Magnetization. *ApJ* 911, 37. doi:10.3847/1538-4357/abea18

Hu, Y., Yuen, K. H., Lazarian, V., Ho, K. W., Benjamin, R. A., Hill, A. S., et al. (2019). Magnetic field morphology in interstellar clouds with the velocity gradient technique. *Nature Astronomy* 3, 776–782. doi:10.1038/s41550-019-0769-0

Hwang, J., Kim, J., Pattle, K., Kwon, W., Sadavoy, S., Koch, P. M., et al. (2021). The JCMT BISTRO Survey: The Distribution of Magnetic Field Strengths toward the OMC-1 Region. *ApJ* 913, 85. doi:10.3847/1538-4357/abf3c4

Inoue, T. and Fukui, Y. (2013). Formation of Massive Molecular Cloud Cores by Cloud-Cloud Collision. *ApJ* 774, L31. doi:10.1088/2041-8205/774/2/L31

Inoue, T., Hennebelle, P., Fukui, Y., Matsumoto, T., Iwasaki, K., and Inutsuka, S.-i. (2018). The formation of massive molecular filaments and massive stars triggered by a magnetohydrodynamic shock wave. *PASJ* 70, S53. doi:10.1093/pasj/psx089

Inutsuka, S.-i., Inoue, T., Iwasaki, K., and Hosokawa, T. (2015). The formation and destruction of molecular clouds and galactic star formation. An origin for the cloud mass function and star formation efficiency. *A&A* 580, A49. doi:10.1051/0004-6361/201425584

Inutsuka, S.-I., Inoue, T., Iwasaki, K., Hosokawa, T., and Kobayashi, M. I. N. (2016). The Formation and Destruction of Molecular Clouds and Galactic Star Formation. In *From Interstellar Clouds to Star-Forming Galaxies: Universal Processes?*, eds. P. Jablonka, P. André, and F. van der Tak. vol. 315, 61–68. doi:10.1017/S1743921316007262

Iwasaki, K., Tomida, K., Inoue, T., and Inutsuka, S.-i. (2019). The Early Stage of Molecular Cloud Formation by Compression of Two-phase Atomic Gases. *ApJ* 873, 6. doi:10.3847/1538-4357/ab02ff

Jaffe, T. R. (2019). Practical Modeling of Large-Scale Galactic Magnetic Fields: Status and Prospects. *Galaxies* 7, 52. doi:10.3390/galaxies7020052

Jansson, R. and Farrar, G. R. (2012a). A New Model of the Galactic Magnetic Field. *ApJ* 757, 14. doi:10.1088/0004-637X/757/1/14

Jansson, R. and Farrar, G. R. (2012b). The Galactic Magnetic Field. *ApJ* 761, L11. doi:10.1088/2041-8205/761/1/L11

Kainulainen, J., Beuther, H., Henning, T., and Plume, R. (2009). Probing the evolution of molecular cloud structure. From quiescence to birth. *A&A* 508, L35–L38. doi:10.1051/0004-6361/200913605

Kandori, R., Tamura, M., Saito, M., Tomisaka, K., Matsumoto, T., Kusakabe, N., et al. (2020a). Distortion of magnetic fields in Barnard 68. *PASJ* 72, 8. doi:10.1093/pasj/psz127

Kandori, R., Tamura, M., Saito, M., Tomisaka, K., Matsumoto, T., Tazaki, R., et al. (2020b). Distortion of Magnetic Fields in the Dense Core CB81 (L1774, Pipe 42) in the Pipe Nebula. *ApJ* 890, 14. doi:10.3847/1538-4357/ab67c5

Kandori, R., Tamura, M., Tomisaka, K., Nakajima, Y., Kusakabe, N., Kwon, J., et al. (2017). Distortion of Magnetic Fields in a Starless Core II: 3D Magnetic Field Structure of FeSt 1-457. *ApJ* 848, 110. doi:10.3847/1538-4357/aa8d18

Kandori, R., Tomisaka, K., Saito, M., Tamura, M., Matsumoto, T., Tazaki, R., et al. (2020c). Distortion of Magnetic Fields in a Starless Core. VI. Application of Flux Freezing Model and Core Formation of FeSt 1-457. *ApJ* 888, 120. doi:10.3847/1538-4357/ab6081

Kim, C.-G. and Ostriker, E. C. (2015). MOMENTUM INJECTION BY SUPERNOVAE IN THE INTERSTELLAR MEDIUM. *The Astrophysical Journal* 802, 99. doi:10.1088/0004-637x/802/2/99

King, P. K., Chen, C.-Y., Fissel, L. M., and Li, Z.-Y. (2019). Effects of grain alignment efficiency on synthetic dust polarization observations of molecular clouds. *MNRAS* 490, 2760–2778. doi:10.1093/mnras/stz2628

King, P. K., Fissel, L. M., Chen, C.-Y., and Li, Z.-Y. (2018). Modelling dust polarization observations of molecular clouds through MHD simulations. *MNRAS* 474, 5122–5142. doi:10.1093/mnras/stx3096

Kounkel, M. and Covey, K. (2019). Untangling the Galaxy. I. Local Structure and Star Formation History of the Milky Way. *AJ* 158, 122. doi:10.3847/1538-3881/ab339a

Kounkel, M., Deng, T., and Stassun, K. G. (2022). Dynamical star forming history of Per OB2. *arXiv e-prints* , arXiv:2206.04703

Krumholz, M. R. and Federrath, C. (2019). The Role of Magnetic Fields in Setting the Star Formation Rate and the Initial Mass Function. *Frontiers in Astronomy and Space Sciences* 6, 7. doi:10.3389/fspas.2019.00007

Kwon, W., Pattle, K., Sadavoy, S., Hull, C. L. H., Johnstone, D., Ward-Thompson, D., et al. (2022). B-fields in Star-forming Region Observations (BISTRO): Magnetic Fields in the Filamentary Structures of Serpens Main. *ApJ* 926, 163. doi:10.3847/1538-4357/ac4bbe

Lazarian, A. (2007). Tracing magnetic fields with aligned grains. *J. Quant. Spec. Radiat. Transf.* 106, 225–256. doi:10.1016/j.jqsrt.2007.01.038

Lazarian, A. and Hoang, T. (2007). Radiative torques: analytical model and basic properties. *MNRAS* 378, 910–946. doi:10.1111/j.1365-2966.2007.11817.x

Lazarian, A. and Yuen, K. H. (2018). Gradients of Synchrotron Polarization: Tracing 3D Distribution of Magnetic Fields. *ApJ* 865, 59. doi:10.3847/1538-4357/aad3ca

Li, H.-b. and Houde, M. (2008). Probing the Turbulence Dissipation Range and Magnetic Field Strengths in Molecular Clouds. *ApJ* 677, 1151–1156. doi:10.1086/529581

Lombardi, M., Bouy, H., Alves, J., and Lada, C. J. (2014). Herschel-Planck dust optical-depth and column-density maps. I. Method description and results for Orion. *A&A* 566, A45. doi:10.1051/0004-6361/201323293

Luri, X., Brown, A. G. A., Sarro, L. M., Arenou, F., Bailer-Jones, C. A. L., Castro-Ginard, A., et al. (2018). Gaia Data Release 2. Using Gaia parallaxes. *A&A* 616, A9. doi:10.1051/0004-6361/201832964

Mouschovias, T. C. and Tassis, K. (2010). Self-consistent analysis of OH-Zeeman observations: too much noise about noise. *MNRAS* 409, 801–807. doi:10.1111/j.1365-2966.2010.17345.x

Ngoc, N. B., Diep, P. N., Parsons, H., Pattle, K., Hoang, T., Ward-Thompson, D., et al. (2021). Observations of Magnetic Fields Surrounding LkHα 101 Taken by the BISTRO Survey with JCMT-POL-2. *ApJ* 908, 10. doi:10.3847/1538-4357/abd0fc

Noutsos, A. (2012). The Magnetic Field of the Milky Way from Faraday Rotation of Pulsars and Extragalactic Sources. *Space Sci. Rev.* 166, 307–324. doi:10.1007/s11214-011-9860-2

Ostriker, E. C., Stone, J. M., and Gammie, C. F. (2001). Density, Velocity, and Magnetic Field Structure in Turbulent Molecular Cloud Models. *ApJ* 546, 980–1005. doi:10.1086/318290

Panopoulou, G. V., Tassis, K., Skalidis, R., Blinov, D., Liodakis, I., Pavlidou, V., et al. (2019). Demonstration of Magnetic Field Tomography with Starlight Polarization toward a Diffuse Sightline of the ISM. *ApJ* 872, 56. doi:10.3847/1538-4357/aafdb2

Pattle, K. and Fissel, L. (2019). Submillimeter and Far-infrared Polarimetric Observations of Magnetic Fields in Star-Forming Regions. *Frontiers in Astronomy and Space Sciences* 6, 15. doi:10.3389/fspas.2019.00015

Pattle, K., Fissel, L., Tahani, M., Liu, T., and Ntormousi, E. (2022). Magnetic fields in star formation: from clouds to cores. *arXiv e-prints* , arXiv:2203.11179

Pattle, K., Lai, S.-P., Wright, M., Coudé, S., Plambeck, R., Hoang, T., et al. (2021). OMC-1 dust polarization in ALMA Band 7: diagnosing grain alignment mechanisms in the vicinity of Orion Source I. *MNRAS* 503, 3414–3433. doi:10.1093/mnras/stab608

Pereyra, A. and Magalhães, A. M. (2007). Polarimetry toward the IRAS Vela Shell. II. Extinction and Magnetic Fields. *ApJ* 662, 1014–1023. doi:10.1086/517906

Pillai, T., Kauffmann, J., Wiesemeyer, H., and Menten, K. M. (2016). CN Zeeman and dust polarization in a high-mass cold clump. *A&A* 591, A19. doi:10.1051/0004-6361/201527803

Pineda, J. E., Schmiedeke, A., Caselli, P., Stahler, S. W., Frayer, D. T., Church, S. E., et al. (2021). Neutral versus Ion Line Widths in Barnard 5: Evidence for Penetration by Magnetohydrodynamic Waves. *ApJ* 912, 7. doi:10.3847/1538-4357/abebdd

Planck Collaboration, Ade, P. A. R., Aghanim, N., Alves, M. I. R., Arnaud, M., Arzoumanian, D., et al. (2016). Planck intermediate results. XXXV. Probing the role of the magnetic field in the formation of structure in molecular clouds. *A&A* 586, A138. doi:10.1051/0004-6361/201525896

Poggio, E., Drimmel, R., Andrae, R., Bailer-Jones, C. A. L., Fouesneau, M., Lattanzi, M. G., et al. (2020). Evidence of a dynamically evolving Galactic warp. *Nature Astronomy* 4, 590–596. doi:10.1038/s41550-020-1017-3

Reich, W., Fürst, E., Reich, P., Wielebinski, R., and Wolleben, M. (2002). Polarization surveys of the galaxy. In *Astrophysical Polarized Backgrounds*, eds. S. Cecchini, S. Cortiglioni, R. Sault, and C. Sbarra. vol. 609 of *American Institute of Physics Conference Series*, 3–8. doi:10.1063/1.1471815

Rezaei Kh., S., Bailer-Jones, C. A. L., Soler, J. D., and Zari, E. (2020). Detailed 3D structure of Orion A in dust with Gaia DR2. *A&A* 643, A151. doi:10.1051/0004-6361/202038708

Rezaei Kh., S. and Kainulainen, J. (2022). Three-dimensional Shape Explains Star Formation Mystery of California and Orion A. *ApJ* 930, L22. doi:10.3847/2041-8213/ac67db

Robishaw, T., Green, J., Surcis, G., Vlemmings, W. H. T., Richards, A. M. S., Etoka, S., et al. (2015). Measuring Magnetic Fields Near and Far with the SKA via the Zeeman Effect. In *Advancing Astrophysics with the Square Kilometre Array (AASKA14)*. 110

Ruiz-Lara, T., Gallart, C., Bernard, E. J., and Cassisi, S. (2020). The recurrent impact of the Sagittarius dwarf on the star formation history of the Milky Way. *Nature Astronomy* 4, 965–973. doi:10.1038/s41550-020-1097-0

Seifried, D. and Walch, S. (2015). The impact of turbulence and magnetic field orientation on star-forming filaments. *MNRAS* 452, 2410–2422. doi:10.1093/mnras/stv1458

Skalidis, R., Sternberg, J., Beattie, J. R., Pavlidou, V., and Tassis, K. (2021a). Why take the square root? An assessment of interstellar magnetic field strength estimation methods. *A&A* 656, A118. doi:10.1051/0004-6361/202142045

Skalidis, R. and Tassis, K. (2021). High-accuracy estimation of magnetic field strength in the interstellar medium from dust polarization. *A&A* 647, A186. doi:10.1051/0004-6361/202039779

Skalidis, R., Tassis, K., Panopoulou, G. V., Pineda, J. L., Gong, Y., Mandarakas, N., et al. (2021b). HI-H_2 transition: exploring the role of the magnetic field. *arXiv e-prints* , arXiv:2110.11878

Soler, J. D. (2019). Using Herschel and Planck observations to delineate the role of magnetic fields in molecular cloud structure. *A&A* 629, A96. doi:10.1051/0004-6361/201935779

Soler, J. D., Ade, P. A. R., Angilè, F. E., Ashton, P., Benton, S. J., Devlin, M. J., et al. (2017). The relation between the column density structures and the magnetic field orientation in the Vela C molecular complex. *A&A* 603, A64. doi:10.1051/0004-6361/201730608

Soler, J. D., Bracco, A., and Pon, A. (2018). The magnetic environment of the Orion-Eridanus superbubble as revealed by Planck. *A&A* 609, L3. doi:10.1051/0004-6361/201732203

Soler, J. D. and Hennebelle, P. (2017). What are we learning from the relative orientation between density structures and the magnetic field in molecular clouds? *A&A* 607, A2. doi:10.1051/0004-6361/201731049

Soubiran, C., Jasniewicz, G., Chemin, L., Zurbach, C., Brouillet, N., Panuzzo, P., et al. (2018). Gaia Data Release 2. The catalogue of radial velocity standard stars. *A&A* 616, A7. doi:10.1051/0004-6361/201832795

Stephens, I. W., Looney, L. W., Dowell, C. D., Vaillancourt, J. E., and Tassis, K. (2011). The Galactic Magnetic Field's Effect in Star-forming Regions. *ApJ* 728, 99. doi:10.1088/0004-637X/728/2/99

Stone, J. M., Gardiner, T. A., Teuben, P., Hawley, J. F., and Simon, J. B. (2008). Athena: A New Code for Astrophysical MHD. *ApJS* 178, 137–177. doi:10.1086/588755

Sullivan, C. H., Fissel, L. M., King, P. K., Chen, C. Y., Li, Z. Y., and Soler, J. D. (2021). Characterizing the magnetic fields of nearby molecular clouds using submillimeter polarization observations. *MNRAS* 503, 5006–5024. doi:10.1093/mnras/stab596

Tahani, M., Glover, J., Lupypciw, W., West, J. L., Kothes, R., Plume, R., et al. (2022a). Orion A's complete 3D magnetic field morphology. *A&A* 660, L7. doi:10.1051/0004-6361/202243322

Tahani, M., Lupypciw, W., Glover, J., Plume, R., West, J. L., Kothes, R., et al. (2022b). 3D magnetic field morphology of the Perseus molecular cloud. *arXiv e-prints* , arXiv:2201.04718

Tahani, M., Plume, R., Brown, J. C., and Kainulainen, J. (2018). Helical magnetic fields in molecular clouds?. A new method to determine the line-of-sight magnetic field structure in molecular clouds. *A&A* 614, A100. doi:10.1051/0004-6361/201732219

Tahani, M., Plume, R., Brown, J. C., Soler, J. D., and Kainulainen, J. (2019). Could bow-shaped magnetic morphologies surround filamentary molecular clouds?. The 3D magnetic field structure of Orion-A. *A&A* 632, A68. doi:10.1051/0004-6361/201936280

Tang, K. S., Li, H.-B., and Lee, W.-K. (2018). Probing the Turbulence Dissipation Range and Magnetic Field Strengths in Molecular Clouds. II. Directly Probing the Ion-neutral Decoupling Scale. *ApJ* 862, 42. doi:10.3847/1538-4357/aacb82

Tassis, K., Ramaprakash, A. N., Readhead, A. C. S., Potter, S. B., Wehus, I. K., Panopoulou, G. V., et al. (2018). PASIPHAE: A high-Galactic-latitude, high-accuracy optopolarimetric survey. *arXiv e-prints* , arXiv:1810.05652

Taylor, A. R., Stil, J. M., and Sunstrum, C. (2009). A Rotation Measure Image of the Sky. *ApJ* 702, 1230–1236. doi:10.1088/0004-637X/702/2/1230

Tritsis, A. and Tassis, K. (2018). Magnetic seismology of interstellar gas clouds: Unveiling a hidden dimension. *Science* 360, 635–638. doi:10.1126/science.aao1185

Van Eck, C. L., Haverkorn, M., Alves, M. I. R., Beck, R., de Bruyn, A. G., Enßlin, T., et al. (2017). Faraday tomography of the local interstellar medium with LOFAR: Galactic foregrounds towards IC 342. *A&A* 597, A98. doi:10.1051/0004-6361/201629707

Voshchinnikov, N. V. (2012). Interstellar extinction and interstellar polarization: Old and new models. *J. Quant. Spec. Radiat. Transf.* 113, 2334–2350. doi:10.1016/j.jqsrt.2012.06.013

Wolleben, M. and Reich, W. (2004). Modelling Faraday Screens in the Interstellar Medium. In *The Magnetized Interstellar Medium*, eds. B. Uyaniker, W. Reich, and R. Wielebinski. 99–104

Wyrzykowski, Ł., Mróz, P., Rybicki, K. A., Gromadzki, M., Kołaczkowski, Z., Zieliński, M., et al. (2020). Full orbital solution for the binary system in the northern Galactic disc microlensing event Gaia16aye. *A&A* 633, A98. doi:10.1051/0004-6361/201935097

Yan, H., Gry, C., Boulanger, F., and Leone, F. (2019). Precision measurement of magnetic field from near to far, from fine to large scales in ISM. *BAAS* 51, 217

Yan, H. and Lazarian, A. (2005). Optical Polarization from Aligned Atoms as a New Diagnostic of Astrophysical Magnetic fields. In *Astronomical Polarimetry: Current Status and Future Directions*, eds. A. Adamson, C. Aspin, C. Davis, and T. Fujiyoshi. vol. 343 of *Astronomical Society of the Pacific Conference Series*, 346

Yan, H. and Lazarian, A. (2006). Polarization of Absorption Lines as a Diagnostics of Circumstellar, Interstellar, and Intergalactic Magnetic Fields: Fine-Structure Atoms. *ApJ* 653, 1292–1313. doi:10.1086/508704

Yan, H. and Lazarian, A. (2007). Polarization from Aligned Atoms as a Diagnostic of Circumstellar, Active Galactic Nuclei, and Interstellar Magnetic Fields. II. Atoms with Hyperfine Structure. *ApJ* 657, 618–640. doi:10.1086/510847

Yan, H. and Lazarian, A. (2012). Tracing magnetic fields with ground state alignment. *J. Quant. Spec. Radiat. Transf.* 113, 1409–1428. doi:10.1016/j.jqsrt.2012.03.027

Zari, E., Lombardi, M., Alves, J., Lada, C. J., and Bouy, H. (2016). Herschel-Planck dust optical depth and column density maps. II. Perseus. *A&A* 587, A106. doi:10.1051/0004-6361/201526597

Zhang, Q., Qiu, K., Girart, J. M., Liu, H. B., Tang, Y.-W., Koch, P. M., et al. (2014). Magnetic Fields and Massive Star Formation. *ApJ* 792, 116. doi:10.1088/0004-637X/792/2/116

Zucker, C., Goodman, A., Alves, J., Bialy, S., Koch, E. W., Speagle, J. S., et al. (2021). On the Three-dimensional Structure of Local Molecular Clouds. *ApJ* 919, 35. doi:10.3847/1538-4357/ac1f96

Zucker, C., Goodman, A. A., Alves, J., Bialy, S., Foley, M., Speagle, J. S., et al. (2022). Star formation near the Sun is driven by expansion of the Local Bubble. *Nature* 601, 334–337. doi:10.1038/s41586-021-04286-5